In silico analysis provides insights for patient-specific annuloplasty in Barlow's disease

Hans Martin Aguilera, MSc,[a] Robert Matongo Persson, MD,[b,c] Rune Haaverstad, MD, PhD,[b,c] Bjørn Skallerud, MSc, PhD,[a] Victorien Prot, MSc, PhD,[a] and Stig Urheim, MD, PhD[b,c]

ABSTRACT

Objective: To predict the required mitral annular area reduction in patients with Barlow's disease to obtain a predefined leaflet area index by a novel in silico modeling method.

Methods: Three-dimensional echocardiography was used to create patient-specific mitral valve models of 8 patients diagnosed with Barlow's disease and bileaflet prolapse preoperatively. Six patients were also studied postoperatively in a finite element framework, to quantify the optimal coaptation area index. For the patient-specific finite element analyses, realistic papillary muscle and annular motion are incorporated, also for the in silico annuloplasty analyses. The annuloplasty ring size is reduced moderately until the optimal coaptation area index is achieved for each patient.

Results: The mean mitral annular area at end-diastole was reduced by 58 ± 7% postoperatively ($P < .001$), resulting in a postoperative coaptation area index of 20 ± 5%. To achieve the same coaptation area index with moderate annular reductions and no leaflet resection the annular reduction was 31 ± 6% ($P < .001$).

Conclusions: In silico analysis in selected patients diagnosed with Barlow's disease demonstrates that annuloplasty with only moderate annular reduction may be sufficient to achieve optimal coaptation as compared to conventional surgical procedures. (JTCVS Open 2023;13:95-105)

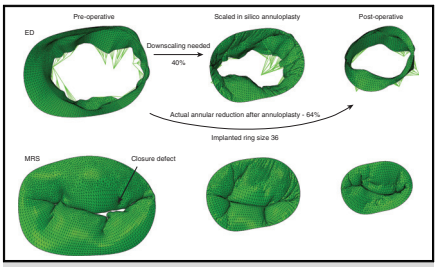

Simulations of moderate annular reductions versus conventional annuloplasty rings.

CENTRAL MESSAGE

In silico analysis by 3D echocardiography has shown that moderate annuloplasty ring scaling secures the same leaflet coaptation area in the individual patient compared with postoperative findings.

PERSPECTIVE

In silico analysis in patients with Barlow's disease demonstrates that annuloplasty with only moderate annular reduction may be sufficient to achieve optimal coaptation as compared with conventional annuloplasty procedures. This novel method may prove helpful in preoperative planning and selection of the ideal annuloplasty ring size.

Video clip is available online.

Degenerative mitral valve diseases such as Barlow's disease (BD) disrupt the already-complex mitral valve anatomy, resulting in mitral regurgitation (MR). BD mitral valves are associated with mitral annular dilation, myxomatous

From the [a]Department of Structural Engineering, Faculty of Engineering Science, The Norwegian University of Science and Technology, Trondheim, Norway; [b]Department of Heart Disease, Haukeland University Hospital, Bergen, Norway; and [c]Department of Clinical Science, Faculty of Medicine, University of Bergen, Bergen, Norway.

This document is the result of the research project funded by the Trond Mohn Foundation (TMS2019TMT09).

Received for publication Jan 17, 2023; accepted for publication Jan 18, 2023; available ahead of print Feb 16, 2023.

Address for reprints: Stig Urheim, MD, PhD, Department of Heart Disease, Haukeland University Hospital, Bergen, Norway (E-mail: stig.urheim@helse-bergen.no).

2666-2736

https://doi.org/10.1016/j.xjon.2023.01.007

Abbreviations and Acronyms

3D = 3-dimensional
BD = Barlow's disease
CAI = coaptation area index
ED = end diastole
FE = finite element
LS = late systole
MAD = mitral annular disjunction
MR = mitral regurgitation
MRS = mitral regurgitation start

thickening, excess of leaflet tissue, leaflet billowing, late systolic regurgitation, a diminished annular saddle shape, and often mitral annular disjunction (MAD).[1-5] Repair strategies used in BD vary and are frequently discussed among surgeons. The goal of every repair is to obtain a good coaptation as well as optimal stress distribution of the leaflets.

In combination with annuloplasty to constrain the unstable annular structure, Carpentier-type resection techniques are often combined with artificial chordal insertions and may also include chordal transfers, chordal shortening, and edge-to-edge techniques.[1,6,7] Furthermore, modified resection techniques and nonresection repair strategies with artificial chordal insertions and annuloplasty have been presented, and they have demonstrated an equivalent degree of reparability for degenerative MR.[8,9] Moreover, in selected patients with BD and bileaflet prolapse with a central leakage and absence of chordal rupture, ring-only repair has been used with good short-term results.[10-12]

Finite element (FE) simulations provide a method to assess the mechanical behavior of the mitral valve apparatus and have the potential to evaluate outcomes of different surgical techniques on a patient's mitral valve. Creating patient-specific mitral valves based on 3-dimensional (3D) echocardiography enables accurate 3D geometries and boundary conditions for FE analysis. Earlier studies related to FE simulations have been performed on a limited number of patients with simplistic boundary conditions, especially when simulating surgical techniques.[13-17] For patients with BD, the mitral annulus moves paradoxically, causing severe annular dilation in late systole (LS).[18] Consequently, the incorporation of this phenomenon in the FE model is important to simulate the accurate mitral valve response. In previous studies, we have demonstrated the importance of implementing annular and papillary muscle dynamics in the FE models,[19,20] as annular dilation is strongly associated with leaflet separation and the onset of MR. In this paper, we studied 8 patients diagnosed with BD and reduced their annulus by scaling an annuloplasty ring to the desired size without leaflet resections. Thereafter, annular and papillary muscle movements from the postoperative echocardiography were applied to avoid the pathologic dynamics observed preoperatively.

Conventional annuloplasty causes a significant reduction of mitral annular area in patients with BD.[5] Undersized annuloplasty may increase the risk of systolic anterior motion and require excessive excision of leaflet tissue. Thus, the objective of the present study was to explore what annuloplasty ring secures the same leaflet coaptation area in the individual patient compared with postoperative findings by in silico modeling. To the best of our knowledge, no study has ever been performed with a sophisticated in silico annuloplasty approach incorporating accurate postoperative mitral valve dynamics. See Figure 1 for a graphical abstract of the study.

METHODS

Patient Population and Data Acquisition

Eight patients diagnosed with BD were included in the present study, selected from a larger cohort of 25 patients, and studied in an FE framework. The selection criteria for this subgroup of patients with BD were bileaflet prolapse, late systolic MR, and no chordal ruptures. Although not a selection criterion, the included patients also had MAD. There were no signs of chordal ruptures by echocardiography, confirmed by absence of early systolic regurgitation on echo Doppler. None of the included patients had connective tissue diseases. The institutional review board or equivalent ethics committee of Haukeland University Hospital approved the study protocol (2016/1132-8) and publication of data (approval date November 28, 2018). The patient(s) provided informed written consent for the publication of the study data. Among the 8 patients, only 6 underwent surgery. Thus, 6 patients were subject for postoperative analyses.

Echocardiographic Analysis

Echocardiographic examinations were performed preoperatively (n = 8) and postoperatively (n = 6) at Haukeland University Hospital, Bergen, Norway. Two-dimensional and 3D recordings were obtained using a Vivid E9 or E95 ultrasound scanner (GE Healthcare). We obtained 3D full-volume data from the apical position (4V probe; GE Healthcare). Echocardiograms were analyzed using EchoPac BT112 (GE Healthcare). For all measurements, we used the average of 3 repeated measures. Left ventricular volumes and ejection fraction were assessed from 3D full-volume recordings. Left atrial volumes were estimated at end-systole using the biplane area–length method and indexed to body surface area to obtain the left atrial volume index.[21] The MR volume was calculated as the difference between left ventricular gross stroke volume (3D end-diastolic volume − 3D end-systolic volume) and aortic stroke volume by Doppler. MR volumes were then indexed to the body surface area for each patient. MR fraction was calculated as the ratio between MR volume and 3D gross stroke volume, expressed in percentage (%).

FE Study and Simulation Pipeline

The FE models were created by performing manual segmentation of the mitral valve leaflets, mitral annulus, and papillary muscle tips based on 3D echocardiographic recordings in 3D Slicer (see Figure 2, *A*).[22] The mitral valve leaflets were segmented at end diastole (ED), and the annular structure and papillary muscle tips were annotated for all time frames from ED to mitral valve opening, capturing the dynamics of the mitral valve apparatus, for both pre- and postoperative anatomies. The mitral annulus and papillary muscle movements were then implemented as displacement boundary conditions in the FE model. For further details on segmentation, mathematical description of the mechanical properties of BD mitral valve leaflets and chordae tendineae, and simulation setup in ABAQUS Explicit (SIMULIA), the reader is referred to our previous work.[19]

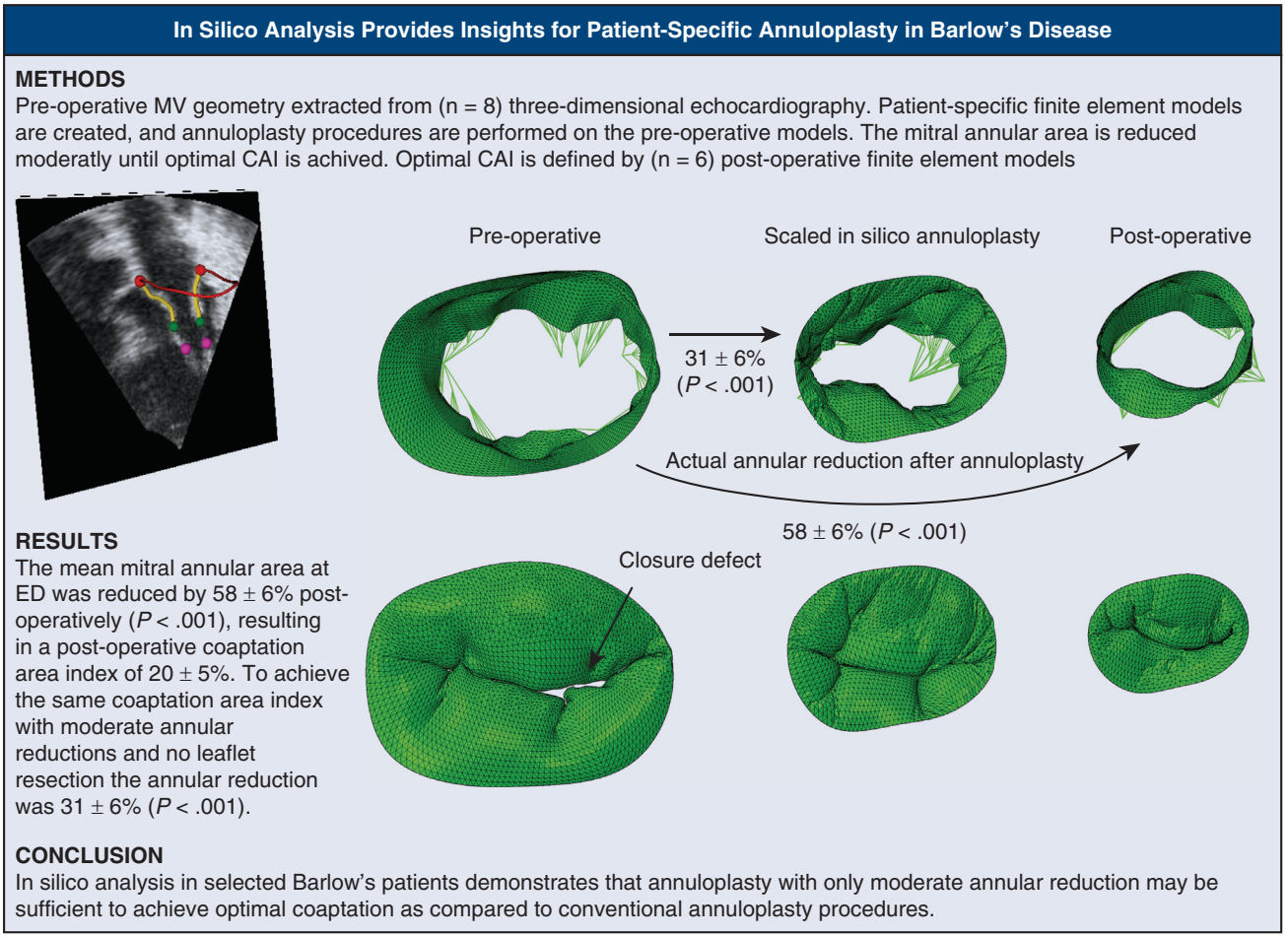

FIGURE 1. Graphical abstract. *MV*, Mitral valve; *CAI*, coaptation area index; *ED*, end diastole.

The in silico annuloplasty procedures were performed by following the pipeline presented in one of our previous reports.[20] In summary, both the pre- and postoperative annular and papillary muscle movements were acquired. Postoperatively, we observed stabilized annular and papillary muscle movements, without annular dilation. Hence, only rigid body annular translations and rotations were implemented in the in silico annuloplasty procedures together with the stabilized papillary muscle movement. The postoperative analyses gave estimates on what the optimal coaptation area index (CAI)[23,24] was for the repaired mitral valves. Then, the segmented annuloplasty ring was aligned with the preoperative anterior horn and trigones and scaled based on a percentage reduction of the preoperative annulus size (Figure 2, *A*). With the annuloplasty ring implanted in silico (*middle panel* in Figure 2, *B*), the mitral annular area was reduced moderately in magnitude until the downscaling of the simulated annuloplasty procedures yielded the same CAI as the postoperative simulation. Examples of preoperative and annuloplasty simulations are presented in Videos 1 and 2, respectively. Each video is shown together with the CAI and the load–amplitude. By implementing the annuloplasty ring in silico, the mitral annulus was stabilized, preventing the late systolic regurgitation observed as a closure defect in Figure 2, *B*. Among the 8 included patients, 2 patients are yet to have surgery; hence, they were without postoperative information. To run in silico annuloplasty procedures on these patients, idealized postoperative annular and papillary muscle movements were established, which served as boundary conditions for the in silico annuloplasty procedures. These idealized movements of the annulus and the papillary muscles were taken as an average of the postoperative measurements performed on the 6 patients recruited in this study with a postoperative assessment. Finally, the idealized behavior was incorporated in the in silico annuloplasty procedure described previously.

Analysis Goal

The goal of the in silico analysis was to achieve the same CAI as the postoperative analysis by only reducing the size of the mitral annulus, thereby performing a virtual ring-only repair. The mitral annular area was reduced by 5% for each in silico analysis until the CAI of the in silico analysis matched the CAI of the postoperative analysis (Figure 2, *B*).

Statistics

The results are presented as mean ± standard deviation. To compare variables, a paired Student *t* test was employed after checking for normality with the Shapiro–Wilk test. All statistical calculation was performed in IBM SPSS Statistics, version 27, for Windows (IBM Corp).

RESULTS

Clinical Data

Preoperative and postoperative hemodynamic data are presented in Table 1. Patient characteristics together with

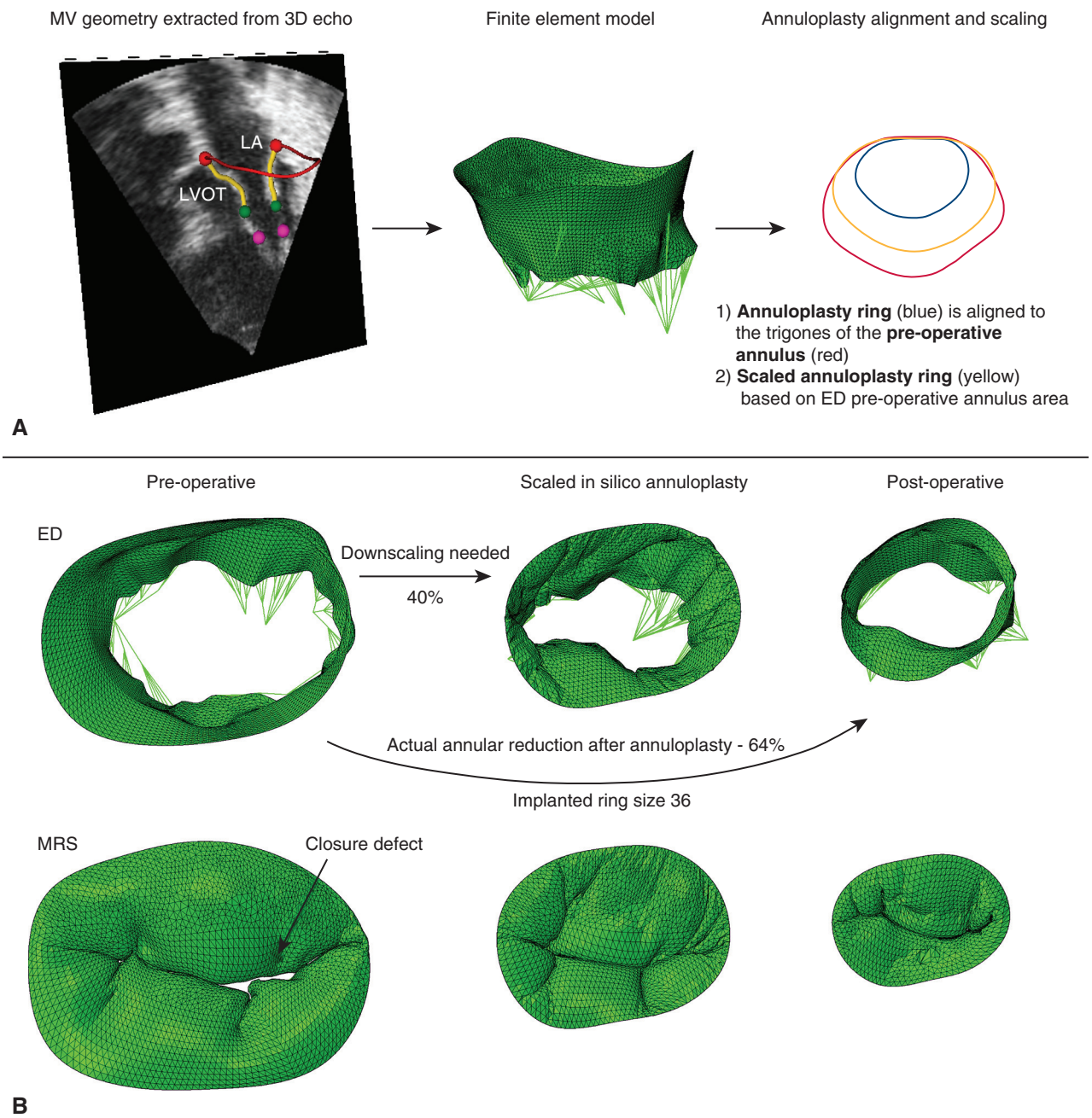

FIGURE 2. A, Echocardiographic extraction of mitral valve geometry, FE model, and in silico annuloplasty procedure. B, Surgeon's view of FE simulation example (patient 6) of preoperative, moderate scaling and postoperative analysis at end diastole (*ED*). *MV*, Mitral valve; *3D*, 3-dimensional; *MRS*, mitral regurgitation start.

intraoperative information on the 6 patients who underwent surgery are presented in Table 2.

Leaflet Coaptation and Annular Dilation

To investigate how annular dilation affected leaflet coaptation, the CAIs of the mitral valve were studied. For each patient, the CAI was the ratio between the leaflet coaptation area and the total segmented leaflet area, expressed as a percentage. Hence, CAI gives an estimate of the mitral valve leaflet area that contributed to coaptation. In Figure 3, the mean preoperative CAI and mean annular area is plotted together with the mean mitral regurgitation start (MRS) for the 8 included patients on a normalized time scale from ED to mitral valve opening. There was a strong time association between the annular dilation increase and the decrease in CAI in LS, with a peak

TABLE 1. Preoperative and postoperative hemodynamic variables for patients with Barlow's disease

Variable	Preoperative (N = 8)	Postoperative (N = 6)	*P* value
HR, beats/min	69 ± 11	71 ± 6	NS
LV-EDV, mL	207 ± 43	159 ± 24	$P = .02$
LV-ESV, mL	78 ± 20	76 ± 17	NS
LV-EF, %	62 ± 5	52 ± 6	$P = .01$
LAV, mL/m^2	67 ± 18	35 ± 5	$P < .001$
RV, mL	59 ± 17	Trace	
RF, %	45 ± 7	Trace	

Values are mean ± SD. *HR*, Heart rate; *NS*, not significant; *LV*, left ventricle; *EDV*, end-diastolic volume; *ESV*, end-systolic volume; *EF*, ejection fraction; *LAV*, left atrial volume index; *RV*, regurgitation volume; *RF*, regurgitation fraction.

TABLE 2. Patient characteristics of the 8 included patients and intraoperative details from the patients who underwent surgery

Patient characteristics	N = 8
Age, y	48 ± 12
Female sex	3 (37.5)
Height, cm	178 ± 8
Weight, kg	77 ± 13
BMI	24.09 ± 3.17
BSA, m^2	1.95 ± 0.2
Heart rate, bpm	71 ± 13
Hypertension	2 (25)
Diabetes mellitus	0
Smoking	0
Atrial fibrillation	2 (25)
Coronary artery disease	0
Intraoperative details	**N = 6**
Ring annuloplasty	6 (100)
Edwards Physio	2 (33.3)
Edwards Physio II	2 (33.3)
Sorin Memo	1 (16.6)
CG Future	1
Posterior leaflet resections	6 (100)
Neo chordae	6 (100)
Chordae transpositions	5 (83.3)

BMI, Body mass index; *BSA*, body surface area.

differentiated CAI and annular dilation curve occurring at a mean of 0.43 ± 0.06 and 0.43 ± 0.04, respectively. Moreover, the late systolic MRS was at 0.39 ± 0.07, showing how annular dilation affect leaflet separation and thus MR.

In all in silico annuloplasty procedures, sufficient coaptation was reached with a scaled annuloplasty ring larger than the implanted ring size postoperatively. For the patients with postoperative analyses (n = 6), the mean actual annular area reduction postoperatively was 58 ± 6% ($P < .001$), whereas the annular reduction required to achieve the same CAI without leaflet resections following in silico annuloplasty was 31 ± 6% ($P < .001$) (see Figure 4, *B*). Moreover, the mean postoperative CAI was 20 ± 5% for the 6 patients at peak systole. For the patients without postoperative echocardiography (patient 7 and 8), the in silico annuloplasty rings was reduced until the 20% CAI threshold was reached. Consequently, the annular reduction of patient 7 was 30%. For patient 8, the required reduction was 40%, which corresponded to the area of a size 38 ring.[25]

In Figure 4, *C*, the mean ± standard deviation curves of the CAI for the scaled in silico annuloplasty procedures and postoperative analyses were presented for the 6 patients. With the in silico annuloplasty procedures initiated at the appropriate scaling, both the in silico analyses and postoperative analyses showed very similar CAI in Figure 4, *C*.

Mitral Valve Leaflet Measurements

In each patient, the segmented mitral valve, both pre- and postoperatively, was measured at ED, as shown in Figure 4, *A* (*right panel*). As demonstrated in the boxplot from Figure 4, *A*, the anterior leaflet lengths were similar in pre- and postoperative recordings, whereas the posterior leaflet lengths were shorter postoperatively due to leaflet resections during surgery. Following resections, the posterior leaflet height in the P2 region was reduced by a mean of 5.4 ± 0.7 mm for the 6 patients ($P < .001$). The mitral annulus was greatly reduced in both the commissural and septolateral dimensions after annuloplasty, with a mean reduction of 30 ± 9% and 39 ± 5% ($P = .002$ and $P < .001$, respectively). Furthermore, the mean segmented leaflet areas were reduced by 36 ± 12% ($P = .003$), and the mean mitral annular area at ED was reduced by 58 ± 7% postoperatively ($P < .001$). Preoperatively, the mitral annulus area was observed to expand by 34 ± 4% ($P < .001$) between ED and LS, whereas the postoperative mitral annular area remained almost constant during the cardiac cycle (Figure 4, *A*, *right panel*). The small fluctuations in postoperative annular area were due to the manual segmentation of the mitral annulus.

The coaptation lengths were measured in A1-P1, A2-P2, and A3-P3 at LS for all analyses (Figure 4, *A*). The preoperative coaptation lengths indicated that there were regions with no coaptation during LS due to lack of closure. When comparing the in silico and postoperative analyses, we found that the coaptation lengths were similar in all regions, demonstrating adequate coaptation for all segments using a repair with moderate annular area reduction and no resection.

Papillary Muscle Forces

For all in silico annuloplasty procedures, there was a reduction in papillary muscle (PM) forces compared

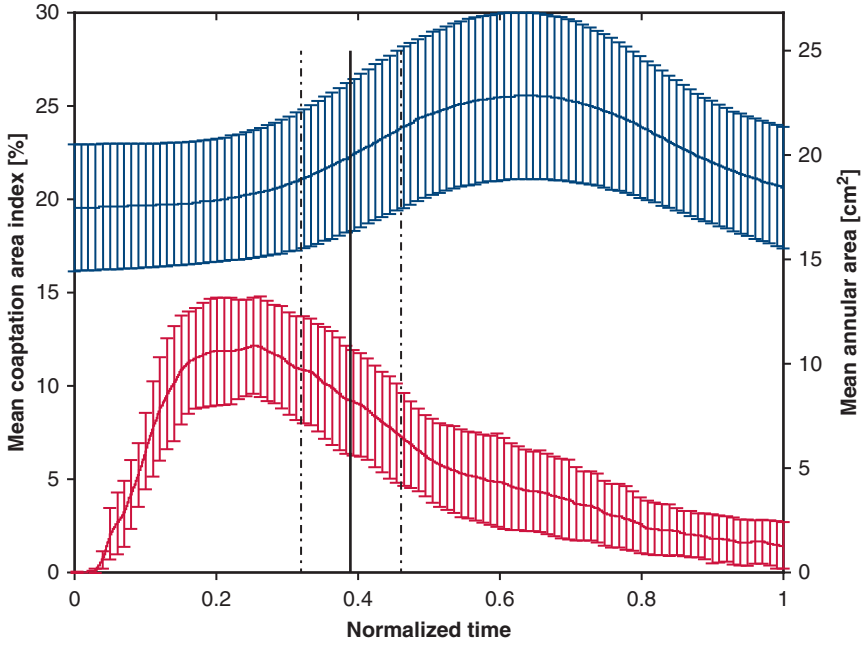

FIGURE 3. Mean ± SD curves of preoperative coaptation and annular area for the included patients from ED to MVO. *Solid black line* displays the mean mitral regurgitation start for the included patients.

with the preoperative analyses (Figure 5, *A*). For the postoperative analyses, there was a decrease in the PM forces, with a mean reduction of 48%, whereas the in silico analyses had a mean reduction of 29%. The mitral annular area is shown to play a role in the forces experienced by the papillary muscles, as a larger annular area requires more leaflet contributing to closure (Figure 5, *B*). The percentage decrease in annular area follows the percentage decrease in PM forces (Figure 5, *A*). The forces reported herein for the postoperative case are in good agreement with our previous study.[26]

Stresses and Strains

The maximum in-plane principal Cauchy stresses and logarithmic strains at peak systole for patient 1 and patient 4 are presented in Figure 6, *A* and *B*, respectively. As demonstrated, annuloplasty aids in reducing stresses in both the anterior and posterior leaflets. In general, there were observed reductions in both stresses and strains after in silico annuloplasty for both leaflets, with the overall greatest reductions observed in the posterior leaflet. After annuloplasty, the posterior leaflet is repositioned anteriorly, causing more of the posterior leaflet to engage in coaptation and increasing the coaptation zone. This results in a smaller pressurized surface toward the atrium leading to reduced PM forces, as discussed in the previous section, and reduced maximum in-plane principal stresses and strains. For patient 1 (Figure 6), this effect is observed for both the anterior and posterior leaflets.

DISCUSSION

In the current study, we use in silico analyses of mitral valves with BD to demonstrate that annuloplasty ring sizes based on moderate annular reductions of the preoperative end-diastolic annular area may be sufficient to achieve optimal coaptation. For a mitral valve with BD experiencing late systolic MR due to annular dilation in the absence of chordal ruptures, based on echocardiographic findings, the insertion of an annuloplasty ring sized to achieve 20% CAI at peak systole may result in successful repair without the need of additional mitral valvuloplasty or chordal insertions.

Surgery of diseased mitral valves with BD commonly includes a combination of highly complex repair strategies, analysis of echocardiographic assessments, and intraoperative observations. Considering that the onset of MR in BD usually occurs in late systole coinciding with annular dilation, leaflets are able to coapt properly in the given pressure regime before annular dilation. Therefore, we claim that valve competence can be achieved by correcting for annular dilation and argue that additional surgical techniques may be a consequence of annular reduction in the setting of excessive tissue. In addition, by not reducing the septolateral diameter as excessively as done with current rings, the risk of systolic anterior motion may diminish as the coaptation zone is displaced toward the posterior orifice.

The method presented could be a beneficial tool when planning complex Barlow's mitral valve surgery. Understanding the dynamics of the mitral valve leaflets, annulus,

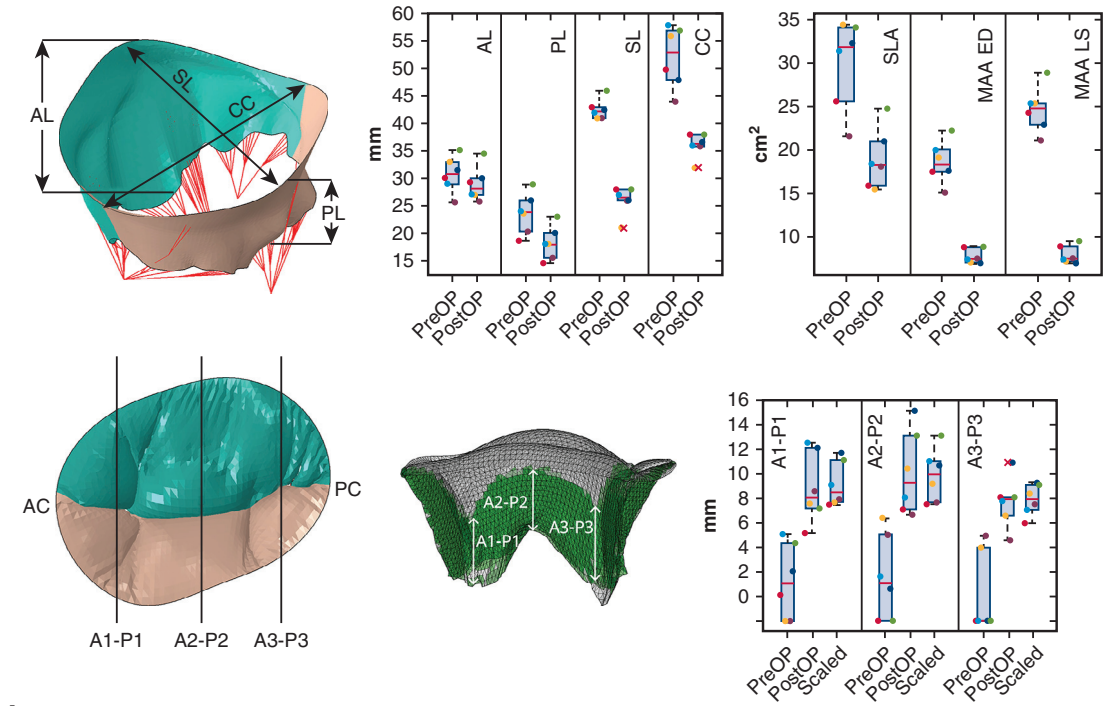

A

Patient	Downscaling	PostOP CAI	PreOP ED MAA [cm^2]	Implanted Ring size	Actual annular reduction
1	25%	11%	17.6	38	54%
2	35%	21%	15.1	38	46%
3	25%	20%	19.1	36	63%
4	25%	27%	17.7	36	59%
5	40%	24%	20	36	64%
6	35%	19%	22.3	38	64%
7	30%	NA	15	NA	NA
8	39%	NA	13.3	NA	NA

B

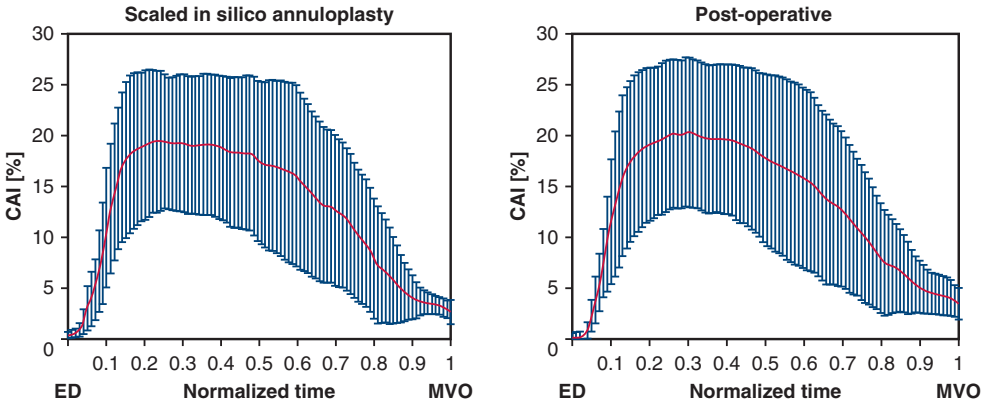

C

FIGURE 4. A, Mitral valve measurements at end diastole (*ED*) for 6 patients with Barlow's disease. Coaptation lengths along the A1-P1, A2-P2, and A3-P3 segments at late systole. For the boxplots, *bottom* and *top* of each box represent the 25th and 75th percentiles, respectively. The *red line* represents the median, and the *whiskers* represent the interquartile range. Outliers are denoted with *red crosses*, and variables in different *colored dots*. B, Magnitude of downscaling in the in silico analyses to obtain the required postoperative coaptation area index (*CAI*), showing the implanted ring size and actual annular reduction following open-heart surgery. C, Leaflet CAI in percentage for the 6 analyses with postoperative and scaled simulations, plotted as mean ± SD. *AL*, Anterior leaflet; *PL*, posterior leaflet; *SL*, septolateral distance; *CC*, intercommissural distance; *SLA*, segmented leaflet area; *MAA*, mitral annular area; *LS*, late systole; *PreOP*, preoperative; *PostOP*, postoperative; *AC*, anterolateral commissure; *PC*, posteromedial commissure; *NA*, not applicable; *MVO*, mitral valve opening.

	AC (PS)	AC (LS)	PC (PS)	PC (LS)	% PM Force reduction	% Annular area reduction
Pre [N]	9.4 ± 1.4	9.8 ± 1.7	11.3 ± 2.6	10.6 ± 2.8	–	–
Post [N]	5.6 ± 1.3	5.4 ± 1.2	5.3 ± 1.6	5.1 ± 1.6	48%	58%
In Silico [N]	8.1 ± 1.4	7.2 ± 2.0	6.7 ± 0.8	6.5 ± 1.0	29%	31%

A

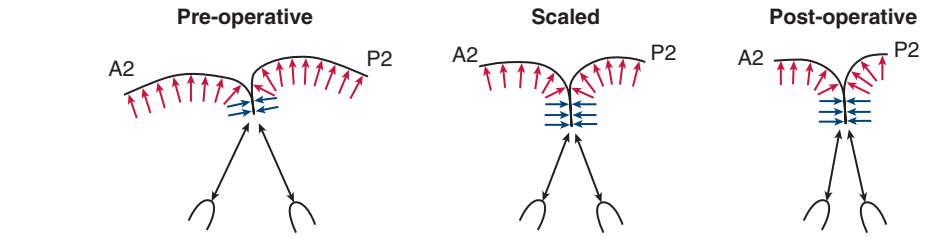

B

FIGURE 5. A, Average papillary muscle forces on the papillary muscle heads in the anterolateral commissure (*AC*) and posteromedial commissure (*PC*) at peak systole (*PS*) and late systole (*LS*). Percentage reduction of preoperative papillary muscle (*PM*) forces and annular area. B, Schematic of force distribution on mitral valve leaflets in systole for a preoperative, scaled and postoperative scenario in systole.

and papillary muscles can provide valuable insights into the preoperative state of the mitral valve. However, there are frequently morphologic features that require additional procedures, such as chordal ruptures or elongations, segmental clefts, and severe excess of posterior leaflet tissue. Furthermore, a severe MAD situation with a history of ventricular arrythmias should be addressed with an appropriate posterior basal leaflet reduction and stabilization of the posterior annular movement. If a mitral valve with BD follows the criteria for ring only repair, the correct annuloplasty ring size can be inserted based on the numerical technique presented in this work. In addition, discovering whether the patient is subject for ring only repair can further facilitate the use of transcatheter annuloplasty procedures in the future.

Stress Distribution and Significance for Results

Although the current study only predicts immediate postoperative results, we demonstrate that optimal annuloplasty adequately reduces maximum in-plane principal stresses and strains. Although the objective of conventional surgery is to abolish any MR and restore valve competency, factors leading to improved long-term results have not been thoroughly investigated. One may argue that the objective of valve competency in surgical repair alone is insufficient, and the objective of mitral repair surgery should not only be to correct for insufficiency, but to create the configuration for coaptation in which there is the most optimal distribution of stress, which may lead to improved long-term results.

Surgical Demographics

As previously mentioned, repair of mitral valve surgery is complex, and mastering such repairs may require a long learning curve and hard-to-come-by hands-on experience. A great number of the procedures are performed at centers with low-to-medium volume of patients (<50 per year). Moreover, minimally invasive strategies in mitral repair are more prevailing in which the portfolio of surgical repair is limited. It is our view that simulation tools in which clinicians can simulate surgical outcomes may not only provide learning but may be able to improve predictability of a repair using minimally invasive techniques or performed outside high-volume centers.

Mitral Annular Dilation and Leaflet Separation

From Figure 3, we observed a strong temporal association between annular dilation, leaflet separation, and MRS. For patients with BD with late systolic MR, this study indicates that at the time point where the mitral annulus dilates the most, the MR starts. It should be noted that the frame-rate of the 3D echocardiographic volume makes it difficult to match the exact time point of MRS as observed with echo Doppler, thus being close in approximation is adequate. For mitral valves with BD with no chordal ruptures and late systolic regurgitation, the preoperative mitral valve is able to prevent regurgitation before mitral annular dilation; hence, moderate annular reductions should enable adequate closure with the native leaflets still intact.

Coaptation Area

In previous studies, the calculation of the coaptation area index is based on echocardiographic measurements, where the coaptation area is measured by defining the coaptation area as the closed leaflet area subtracted from total leaflet area, where the total leaflet area is measured at the onset

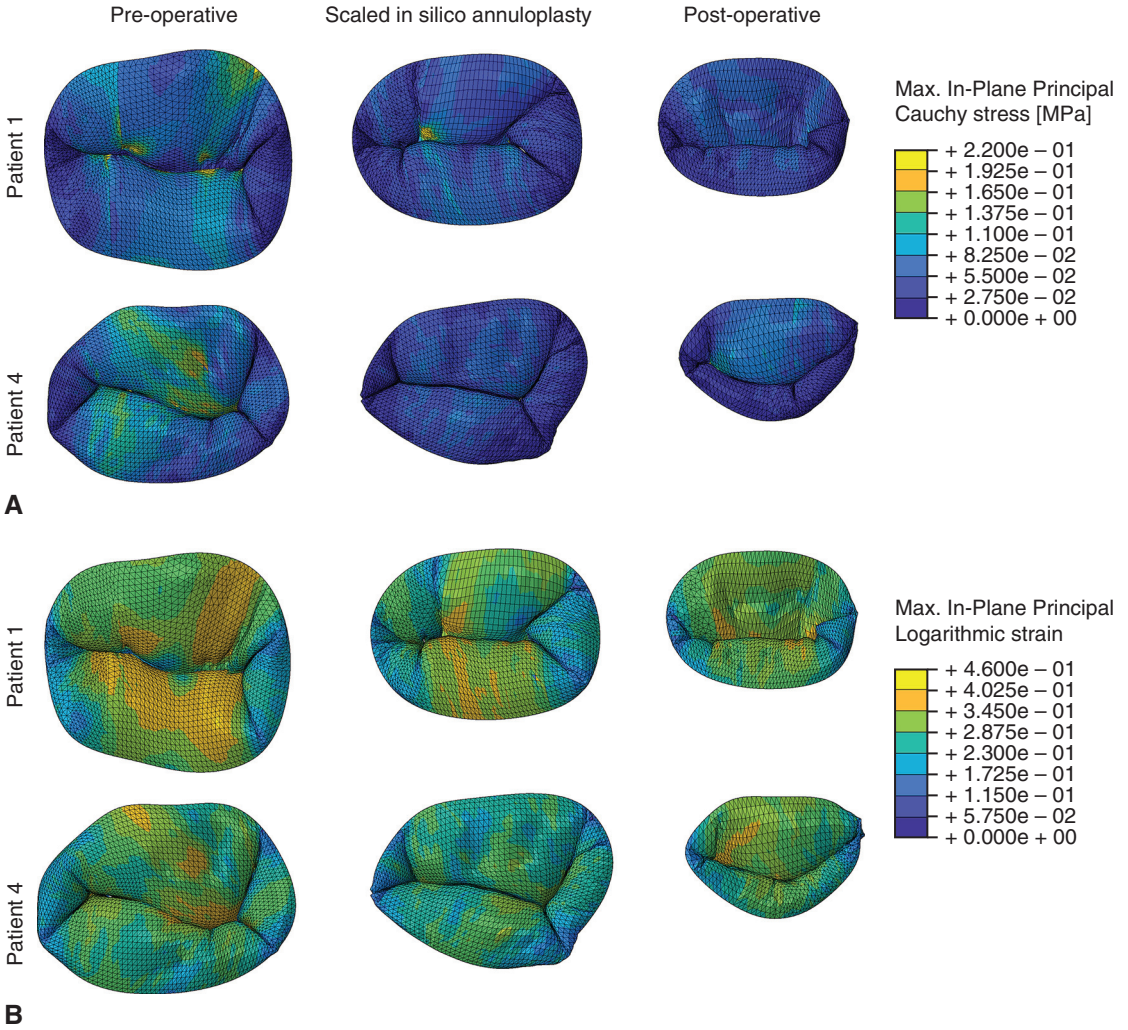

FIGURE 6. A, max in-plane principal stresses for patient 1 and patient 4. B, max in-plane principal lograthimic strains for patient 1 and patient 4.

of mitral valve closure.[23,24] In the present study, the total segmented leaflet area is assessed at ED, and the coaptation area is defined as the total area of elements in contact at any given time point. This provides a more accurate estimate of coaptation area, also including the commissures. In Figure 4, *A*, *right panel*, the segmented leaflet area is observed to be substantially smaller postoperatively with a 36 ± 12% ($P = .003$) decrease, which is a greater decrease in segmented leaflet area than the actual leaflet resected during surgery. It should be noted that the mitral valve leaflets folds after surgery due to the annular reduction, making it difficult to detect these folds on echocardiography. Hence, the segmented leaflet area reduction is likely exaggerated in this study. However, in terms of the coaptation area index, the folded leaflets not accounted for will not affect the results, as the folded leaflet regions are in contact.

Limitations

This study presents a repair strategy for selected patients with BD with certain characteristics, which accurately reproduce the immediate postoperative outcome. However, BD is a dynamic degenerative process, and the analyses presented here are not capable of predicting the long-term outcomes of this repair strategy. As the patients with BD in this study have undergone complex repair and not a ring-only strategy, we are not able to understand the potential drawbacks of ring-only repair where the goal is to achieve sufficient coaptation. Nevertheless, there are indications that ring-only repair can be a good strategy for selected patients.[10-12]

Currently, the presented in silico analyses require a significant amount of manual work in terms of segmentation and simulation setup. Hence, adapting this current pipeline

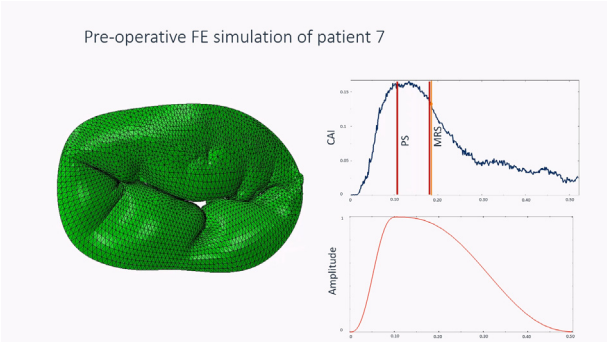

VIDEO 1. Preoperative finite element (FE) simulation with coaptation area index (CAI) and load amplitude. At mitral regurgitation start (MRS), the closure defect is depicted. Peak systole (PS), aortic valve closure (AVC), mitral valve opening (MVO). Video available at: https://www.jtcvs.org/article/S2666-2736(23)00015-3/fulltext.

to clinical practice is at present time-consuming and cumbersome. With the emergence of reliable automated segmentation techniques, the simulation setup can also be automated, which opens for broad clinical use. At the current time, automatic annotation of the mitral annulus and papillary muscle tips throughout the entire cardiac cycle is challenging for mitral valve disease.

The annular movement incorporated in the in silico analyses is based on postoperative echocardiography; hence, we do not account for different annuloplasty ring materials and degrees of rigidity. Current rings on the market are not particularly dynamic, as shown in the recently published paper by Frishman and colleagues[27]; hence, incorporating the annular rigid body translations and rotations are sufficient to model in silico annuloplasty. In the future, we plan to study change in geometry and the elastic behavior of annuloplasty rings with our in silico annuloplasty pipeline. This will enable us to further study the optimal annuloplasty ring for clinical use.

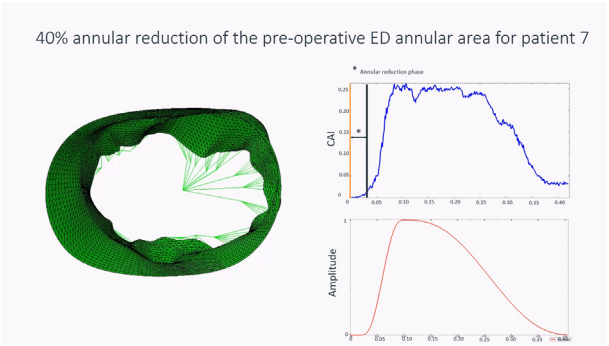

VIDEO 2. In silico finite element (FE) simulation with coaptation area index (CAI) and load amplitude. No closure defect is observed and mitral valve remains closed during systole. End diastole (ED), peak systole (PS), aortic valve closure (AVC), mitral valve opening (MVO). Video available at: https://www.jtcvs.org/article/S2666-2736(23)00015-3/fulltext.

CONCLUSIONS

In the present study, we have showed that with simulation of annuloplasty procedures, we are able to predict the coaptation area postoperatively without leaflet resections. In silico analysis in patients with BD demonstrates that annuloplasty with only moderate annular reduction may be sufficient to achieve optimal coaptation as compared with conventional annuloplasty procedures. Sizing the annular area as a percentage decrease of end-diastolic area may eliminate the risk of systolic anterior motion and reduce the extent of mitral valvuloplasty. This method may prove helpful in preoperative planning and selection of the ideal annuloplasty ring size.

Conflict of Interest Statement

The authors reported no conflicts of interest.

The *Journal* policy requires editors and reviewers to disclose conflicts of interest and to decline handling or reviewing manuscripts for which they may have a conflict of interest. The editors and reviewers of this article have no conflicts of interest.

References

1. Anyanwu AC, Adams DH. Etiologic classification of degenerative mitral valve disease: Barlow's disease and fibroelastic deficiency. *Semin Thorac Cardiovasc Surg*. 2007;19:90-6. https://doi.org/10.1053/j.semtcvs.2007.04.002
2. Apor A, Nagy AI, Kovács A, Manouras A, Andrássy P, Merkely B. Three-dimensional dynamic morphology of the mitral valve in different forms of mitral valve prolapse—potential implications for annuloplasty ring selection. *Cardiovasc Ultrasound*. 2016;14:32. https://doi.org/10.1186/s12947-016-0073-4
3. Barber JE, Kasper FK, Ratliff NB, Cosgrove DM, Griffin BP, Vesely I. Mechanical properties of myxomatous mitral valves. *J Thorac Cardiovasc Surg*. 2001;122:955-62. https://doi.org/10.1067/mtc.2001.117621
4. Hjortnaes J, Keegan J, Bruneval P, Schwartz E, Schoen F, Carpentier A, et al. Comparative histopathological analysis of mitral valves in Barlow disease and fibroelastic Deficiency. *Semin Thorac Cardiovasc Surg*. 2016;28:757-67. https://doi.org/10.1053/j.semtcvs.2016.08.015
5. Maffessanti F, Marsan NA, Tamborini G, Sugeng L, Caiani EG, Gripari P, et al. Quantitative analysis of mitral valve apparatus in mitral valve prolapse before and after annuloplasty: a three-dimensional intraoperative transesophageal study. *J Am Soc Echocardiogr*. 2011;24:405-13. https://doi.org/10.1016/j.echo.2011.01.012
6. Carpentier A. Cardiac valve surgery—the "French correction." *J Thorac Cardiovasc Surg*. 1983;86:323-37. https://doi.org/10.1016/S0022-5223(19)39144-5
7. Maisano F, Torracca L, Oppizzi M, Stefano PL, D'Addario G, La Canna G, et al. The edge-to-edge technique: a simplified method to correct mitral insufficiency. *Eur J Cardiothorac Surg*. 1998;13:240-6. https://doi.org/10.1016/S1010-7940(98)00014-1
8. Lawrie GM, Zoghbi W, Little S, Shah D, Ben-Zekry Z, Earle N, et al. One hundred percent reparability of degenerative mitral regurgitation: intermediate-term results of a dynamic engineered approach. *Ann Thorac Surg*. 2016;101:576-83; discussion 583-4. https://doi.org/10.1016/j.athoracsur.2015.07.029
9. Asai T. The butterfly technique. *Ann Cardiothorac Surg*. 2015;4:370-5. https://doi.org/10.3978/J.ISSN.2225-319X.2015.07.02
10. De Paulis R, Maselli D, Salica A, Leonetti S, Wolf LG, Weltert L, et al. Mitral repair with the sole use of a semi-rigid band in a sub-population of patients with Barlow's disease: a 4-year follow-up with stress echocardiography. *Interact Cardiovasc Thorac Surg*. 2015;21:316-21. https://doi.org/10.1093/icvts/ivv170
11. Ben Zekry S, Spiegelstein D, Sternik L, Lev I, Kogan A, Kuperstein R, et al. Simple repair approach for mitral regurgitation in Barlow disease. *J Thorac Cardiovasc Surg*. 2015;150:1071-7.e1. https://doi.org/10.1016/j.jtcvs.2015.08.023
12. Raanani E, Schwammenthal E, Moshkovitz Y, Cohen H, Kogan A, Peled Y, et al. Repair with annuloplasty only of balanced bileaflet mitral valve prolapse with

severe regurgitation. *Eur J Cardio-Thoracic Surg*. 2022;61:908-16. https://doi.org/10.1093/ejcts/ezab548

13. Stevanella M, Maffessanti F, Conti CA, Votta E, Arnoldi A, Lombardi M, et al. Mitral valve patient-specific finite element modeling from cardiac MRI: application to an annuloplasty procedure. *Cardiovasc Eng Technol*. 2011;2:66-76. https://doi.org/10.1007/s13239-010-0032-4
14. Choi A, McPherson DD, Kim H. Computational virtual evaluation of the effect of annuloplasty ring shape. *Int j numer method biomed eng*. 2017;33:e2831. https://doi.org/10.1002/CNM.2831
15. Votta E, Maisano F, Bolling SF, Alfieri O, Montevecchi FM, Redaelli A. The Geoform disease-specific annuloplasty system: a finite element study. *Ann Thorac Surg*. 2007;84:92-101. https://doi.org/10.1016/j.athoracsur.2007.03.040
16. Kong F, Pham T, Martin C, Elefteriades J, McKay R, Primiano C, et al. Finite element analysis of annuloplasty and papillary muscle relocation on a patient-specific mitral regurgitation model. *PLoS One*. 2018;13:1-15. https://doi.org/10.1371/journal.pone.0198331
17. Sturla F, Onorati F, Votta E, Pechlivanidis K, Stevanella M, Milano AD, et al. Is it possible to assess the best mitral valve repair in the individual patient? Preliminary results of a finite element study from magnetic resonance imaging data. *J Thorac Cardiovasc Surg*. 2014;148:1025-34. https://doi.org/10.1016/J.JTCVS.2014.05.071
18. Dumont KA, Dahl Aguilera HM, Persson R, Prot V, Escobar Kvitting JP, Urheim S. Mitral annular elasticity determines severity of regurgitation in Barlow's mitral valve disease. *J Am Soc Echocardiogr*. 2022;35:1037-46. https://doi.org/10.1016/j.echo.2022.07.001
19. Aguilera HM, Urheim S, Skallerud B, Prot V. Influence of annular dynamics and material behavior in finite element analysis of Barlow's mitral valve disease. *J Elast*. 2021;145:163-90. https://doi.org/10.1007/s10659-021-09829-5
20. Aguilera HM, Urheim S, Persson RM, Haaverstad R, Skallerud B, Prot V. Finite element analysis of mitral valve annuloplasty in Barlow's disease. *J Biomech*. 2022;142:111226. https://doi.org/10.1016/j.jbiomech.2022.111226
21. Lang RM, Bierig M, Devereux RB, Flachskamp FA, Foster E, Pellikka PA, et al. Recommendations for chamber quantification: a report from the American Society of Echocardiography's Guidelines and Standards Committee and the Chamber Quantification Writing Group, developed in conjunction with the European Association of Echocardiography, a branch of the European Society of Cardiology. *J Am Soc Echocardiogr*. 2005;18:1440-63. https://doi.org/10.1016/J.ECHO.2005.10.005
22. Fedorov A, Beichel R, Kalpathy-Cramer J, Finet J, Fillion-Robin J, Pujol S, et al. 3D Slicer as an image computing platform for the Quantitative Imaging Network. *Magn Reson Imaging*. 2012;30:1323-41. https://doi.org/10.1016/J.MRI.2012.05.001
23. Guo Y, He Y, Zhang Y, Shuping G, Sun L, Liu W, et al. Assessment of the mitral valve coaptation zone with 2D and 3D transesophageal echocardiography before and after mitral valve repair. *J Thorac Dis*. 2018;10:283-90. https://doi.org/10.21037/jtd.2017.12.62
24. Saito K, Okura H, Watanabe N, Obase K, Tamada T, Koyama T, et al. Influence of chronic tethering of the mitral valve on mitral leaflet size and coaptation in functional mitral regurgitation. *JACC Cardiovasc Imaging*. 2012;5:337-45. https://doi.org/10.1016/J.JCMG.2011.10.004
25. Carpentier A, Adams D. *Degenerative Valvular Disease Specific Annuloplasty Rings*; 2009.
26. Prot V, Haaverstad R, Skallerud B. Finite element analysis of the mitral apparatus: annulus shape effect and chordal force distribution. *Biomech Model Mechanobiol*. 2009;8:43-55. https://doi.org/10.1007/s10237-007-0116-8
27. Frishman S, Asme M, Kight A, Maddineni S, Imbrie-Moore A, Karachiwalla Z, et al. DynaRing: a patient-specific mitral annuloplasty ring with selective stiffness segments. *J Med*. 2022;16:31009-10. https://doi.org/10.1115/1.4054445

Key Words: annuloplasty, mitral valve, mitral valve regurgitation, finite element analysis, Barlow's disease, patient-specific